Supporting Information

Self-assembled Novel Co/Ni-based ε-Keggin Crystal Materials as Highly Efficient Photocatalysts for Diluted CO_2 Photoreduction

Yin-Hua Zhu[a], Jian-Bo Yang[a], Pin-Fang Yan[a], Zhi-Ming Dong[a], Hua Mei[a,*], Yan Xu[a,b,*]

[a]State Key Laboratory of Materials-Oriented Chemical Engineering, College of Chemical Engineering, Nanjing Tech University, Nanjing, 211816, P.R. China.

[b]State Key Laboratory of Coordination Chemistry, Coordination Chemistry Institute, Nanjing University, Nanjing 210023, P.R. China.

Corresponding Authors

E-mail: yanxu@njtech.edu.cn (Y. Xu); meihua@njtech.edu.cn (H. Mei).

Table of Contents

Fig. S13 (a) Co 2p spectrum analysis of **Co-ε-Keggin**. (b) Mo 3d spectrum analysis of **Co-ε-Keggin**. (c) Full spectrum analysis of **Co-ε-Keggin**. (d) Ni 2p spectrum analysis of **Ni-ε-Keggin**. (e) Mo 3d spectrum analysis of **Ni-ε-Keggin**. (f) Full spectrum analysis of **Ni-ε-Keggin**.

5. Photocatalytic CO_2 reduction experiments

Fig. S14 The photograph of the CO_2 photoreduction devices.

Fig. S15 UV/vis spectra, K-M function curves of **Co-ε-Keggin.**

Fig. S16 Mott-Schottky plots for catalysts **Co-ε-Keggin**.

Fig. S17 Mott-Schottky plots for catalysts **Ni-ε-Keggin**.

Fig. S18 GC profiles of CO_2 reduction to CO without light.

Fig. S19 GC profiles of 10% CO_2 reduction to CO with **Ni-ε-Keggin** as catalyst after reaction 6 h.

Fig. S20 GC profiles of 10% CO_2 reduction to CO with **Co-ε-Keggin** as catalyst after reaction 6 h.

Fig. S21 PXRD patterns of **Co-ε-Keggin** before and after CO_2RR.

Fig. S22 PXRD patterns of **Ni-ε-Keggin** before and after CO_2RR.

Fig. S23 Z- scheme diagram of the electron transfer process by using **Ni-ε-Keggin** as photocatalyst.

Fig. S24 Comparison of the activity of the photocatalytic CO_2RR under different conditions when catalyst **Ni-ε-Keggin** was used.

Fig. S25 K-M function curves of $[Ru(bpy)_3]Cl_2$. Mott-Schottky plots for $[Ru(bpy)_3]Cl_2$.

Fig. S26 CO_2 adsorption isotherms (298 K) of **{Ni_4Mo_{12}}** and **Ni-ε-Keggin** materials.

6. Table

Table S1. Comparison of reported POM-based hybrid materials photocatalyst for pure CO_2 to CO conversion.

Table S2. Comparison of reported POM-based hybrid materials photocatalyst for 10% diluted CO_2 to CO conversion.

Table S3. Selected bond lengths (Å) for **Co-ε-Keggin**.

7. Theoretical calculations

8. References

1. Materials and Physical property studies.

All chemicals were purchased from Aladdin Shanghai without further purification. The **$[Mo^{V}_{12}O_{30}(\mu_2\text{-}OH)_{10}H_2\{Ni^{II}(H_2O)_3\}_4]$** abbreviated to **$\{Ni_4Mo_{12}\}$** was synthesized according to the corresponding literature.[17] The contents of C, H, and N were acquired using a PerkinElmer 2400 element analyzer. FT-IR spectra were conducted on a Nicolet Impact 410 Fourier transform infrared spectrometer from 4000-400 cm^{-1}. Powder X-ray diffraction (PXRD) patterns were performed on a Bruker D8X diffractometer with Cu-Kα (λ=1.5418 Å) radiation at 2θ in the range of 5-50° with a step size of 0.02°. TGA measurements were performed by a Diamond thermogravimetric analyzer under an atmosphere of flowing nitrogen with a heating rate of 10°C min^{-1} from room temperature to 800°C. UV-vis diffuse reflectance spectra (Barium sulfate as reference) were collected on a SHIMADZU UV-2600 spectrophotometer in the range of 200-800 nm. The SEM were identified by using a Hitachi TM 3000 scanning electron microscope at an accelerating voltage of 20 kV. Elemental analyses (C, N and H) were determined by a Perkin-Elmer 2400 elemental analyzer. CO labelled by ^{13}C was performed with gas chromatography-mass spectrometer (Agilent 6890 N/5975, USA).

2. Experimental section

2.1 Electrochemical measurements

The Mott-Schottky spots were carried out in an ambient environment by using the electrochemical workstation (CHI 760e) in a standard three-electrode system: The carbon cloth (CC, 1 cm×1 cm) modified with catalyst samples, carbon rod and Ag/AgCl were used as the working electrode, counter electrode, and the reference electrode, respectively. The catalyst of 2 mg was ground to powder and then dispersed in 1 mL of 0.5% Nafion solvent by ultrasonication to form a homogeneous ink. Subsequently, 200 μL of the ink was deposited onto the carbon cloth and dried at room temperature for Mott-Schottky spots measurements. The Mott-Schottky plots were measured over an alternating current (AC)

frequency of 1000 Hz, 1500 Hz, and 2000 Hz, and three electrodes were immersed in the 0.2 M Na_2SO_4 aqueous solution.

3. Structure

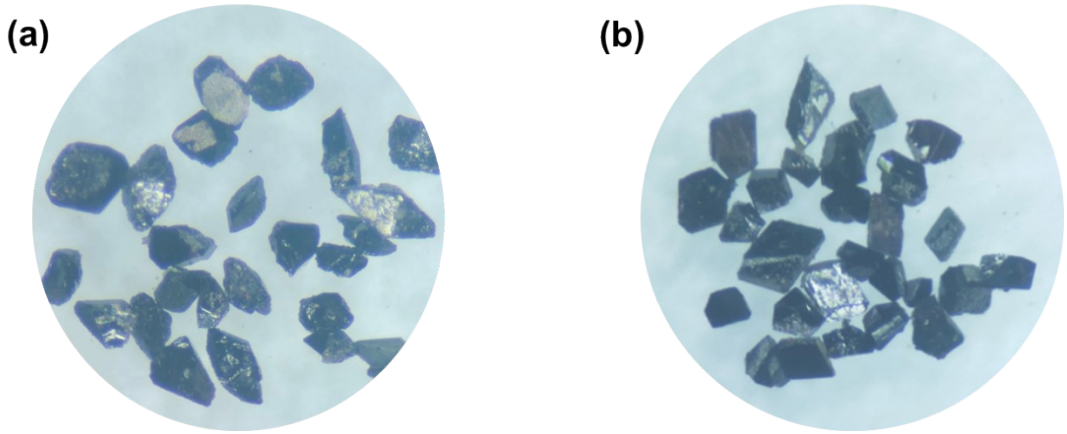

Fig. S1 (a) The view of **Co-ε-Keggin** under an optical microscope. (b) The view of **Ni-ε-Keggin** under an optical microscope.

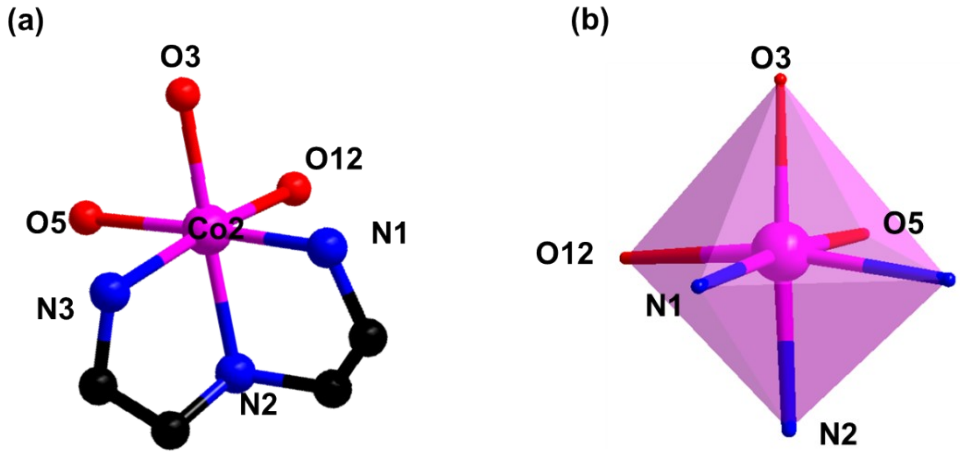

Fig. S2 (a) Ball-and-stick model of Co ion coordination mode. (b) Polyhedron model of Co ion coordination mode.

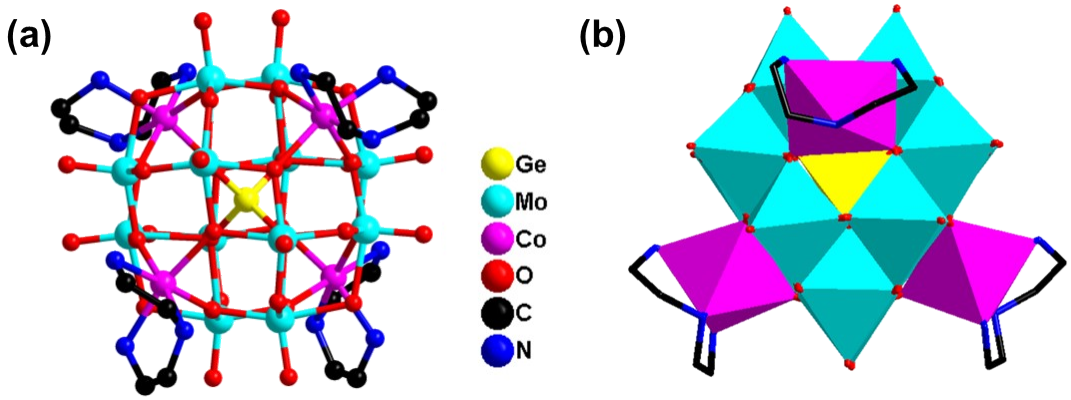

Fig. S3 (a) Ball-and-stick model diagram of **Co-ε-Keggin**. (b) polyhedron model diagram of **Co-ε-Keggin.**

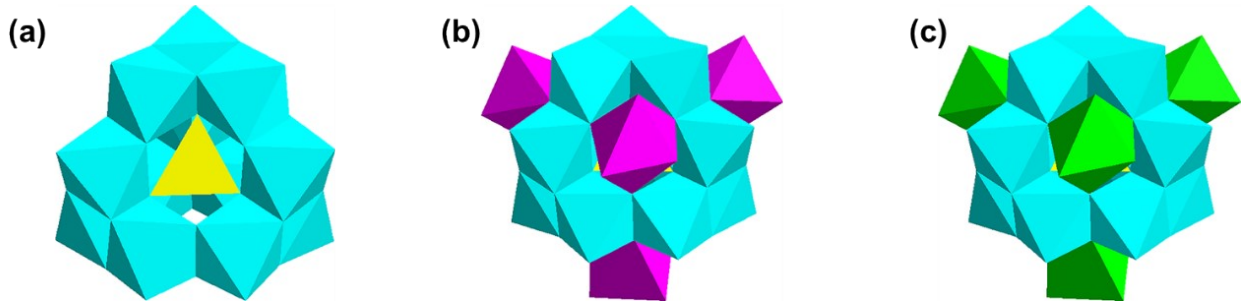

Fig. S4 (a) ε-Keggin polyhedron diagram. (b) Co-ε-Keggin polyhedron diagram. (c) Ni-ε-Keggin polyhedron diagram.

4. Characterizations

4.1 EDS-Mapping

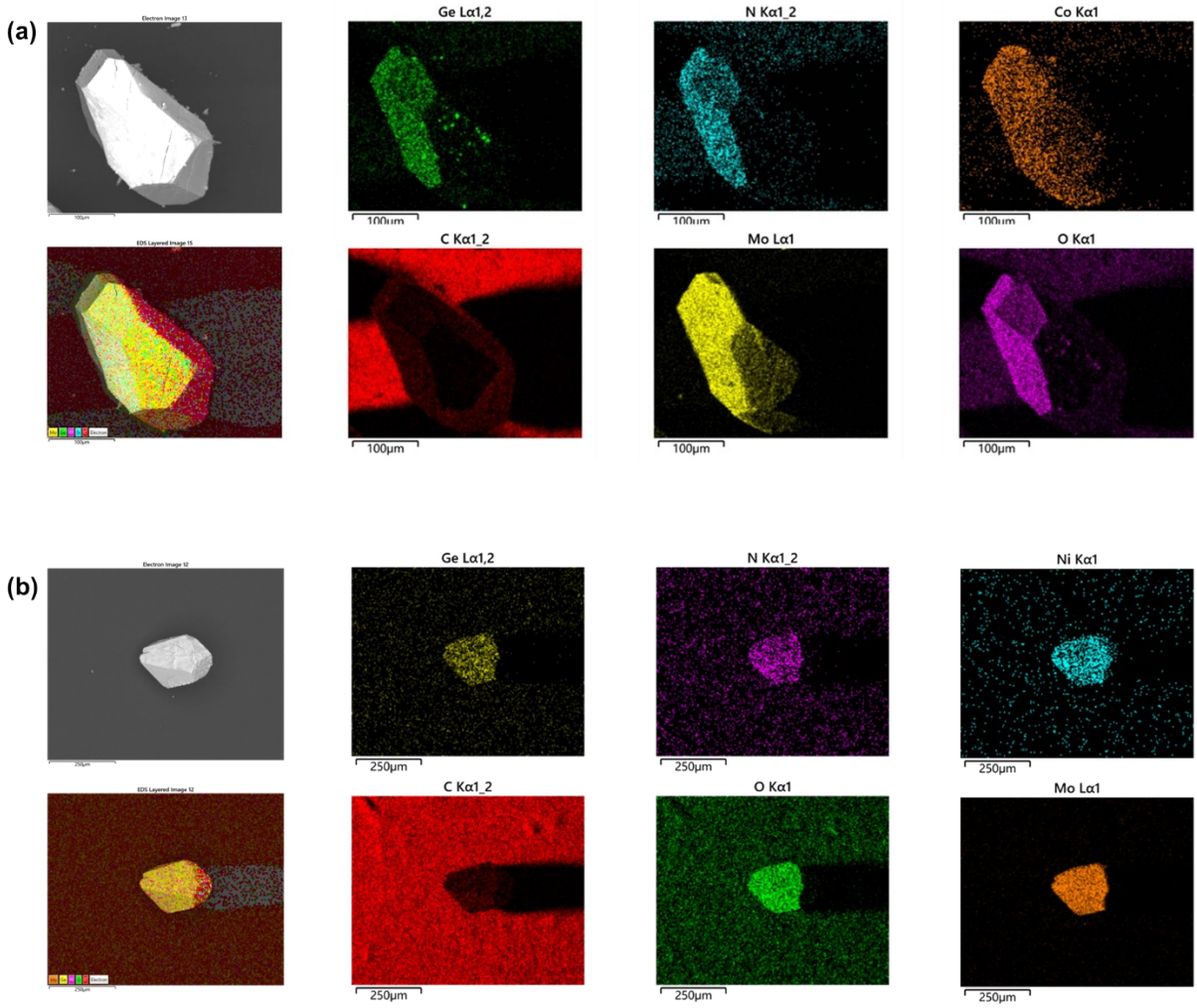

Fig. S5 (a) EDS-mapping diagram of **Co-ε-Keggin**. (b) EDS-mapping of **Ni-ε-Keggin**.

4.2 IR

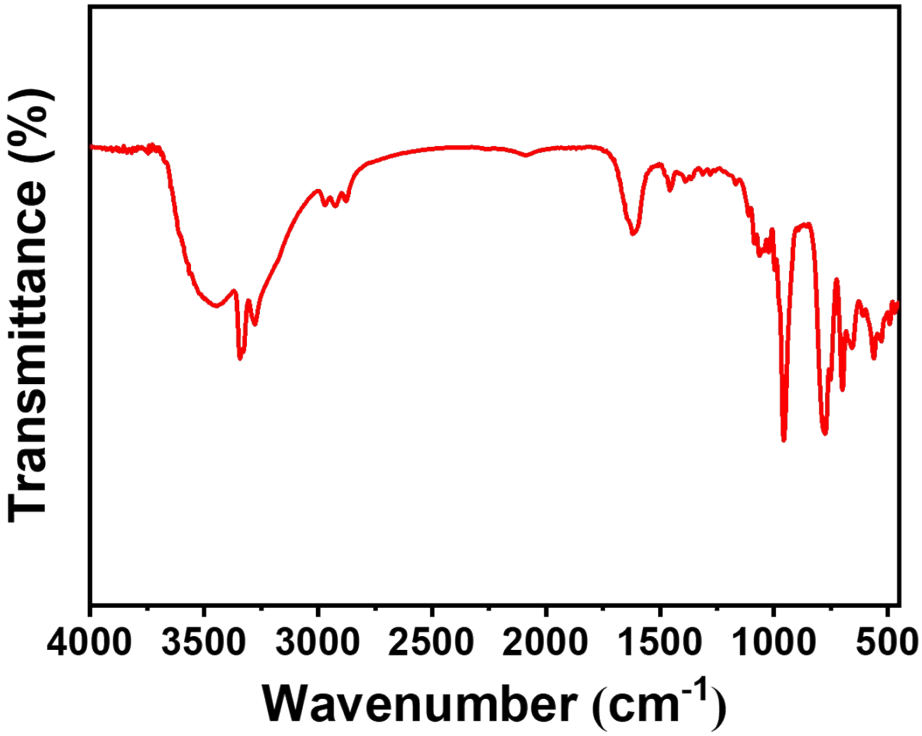

Fig. S6 The IR spectrum of **Co-ε-Keggin.**

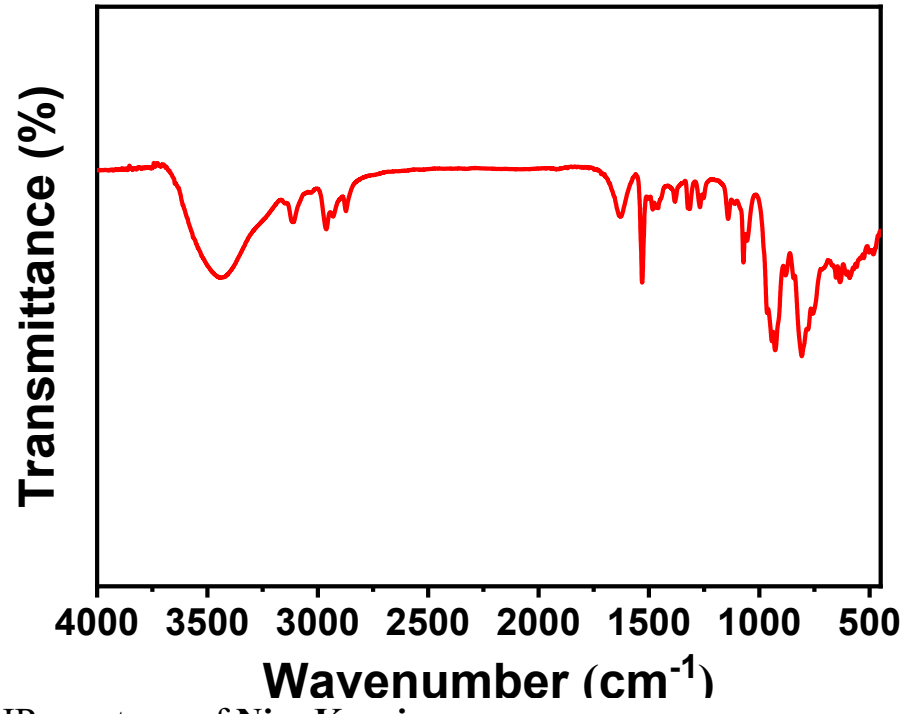

Fig. S7 The IR spectrum of **Ni-ε-Keggin.**

4.3 PXRD patterns

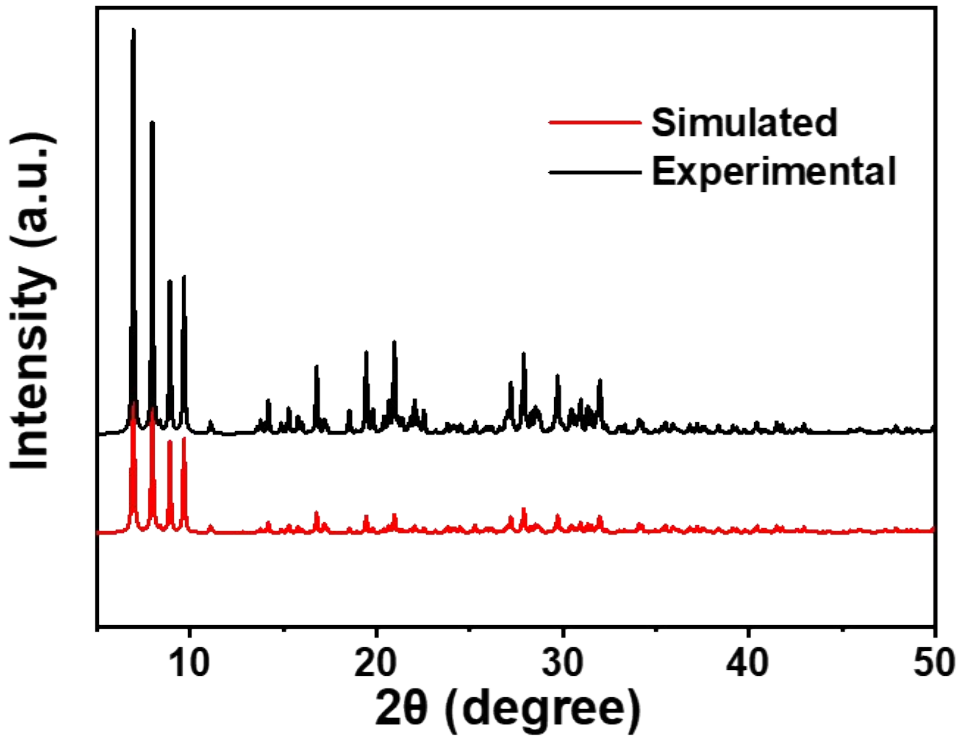

Fig. S8 The experimental and simulated powder PXRD patterns of **Co-ε-Keggin.**

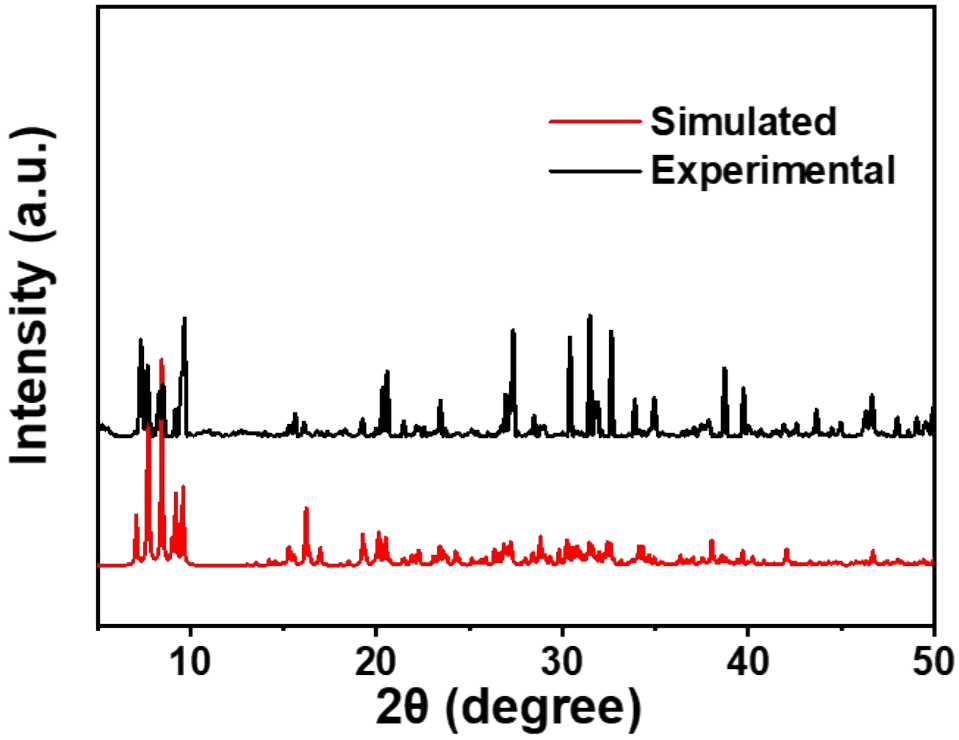

Fig. S9 The experimental and simulated powder PXRD patterns of **Ni-ε-Keggin.**

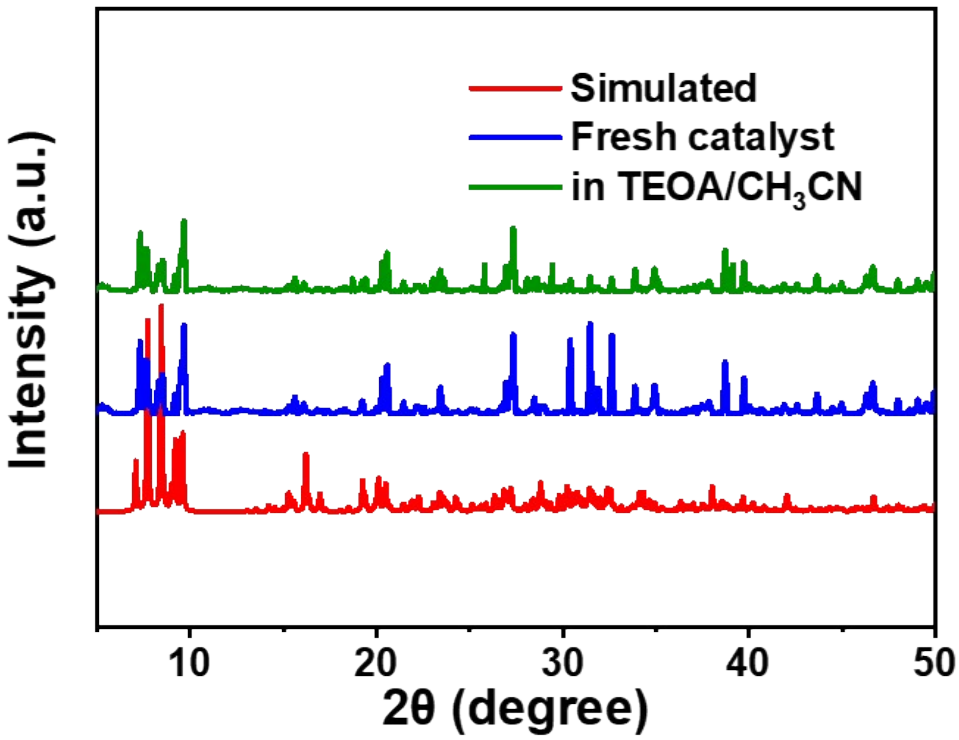

Fig. S10 Solvent stability in TEOA/CH_3CN mixed solvents of **Ni-ε-Keggin.**

4.4 TGA

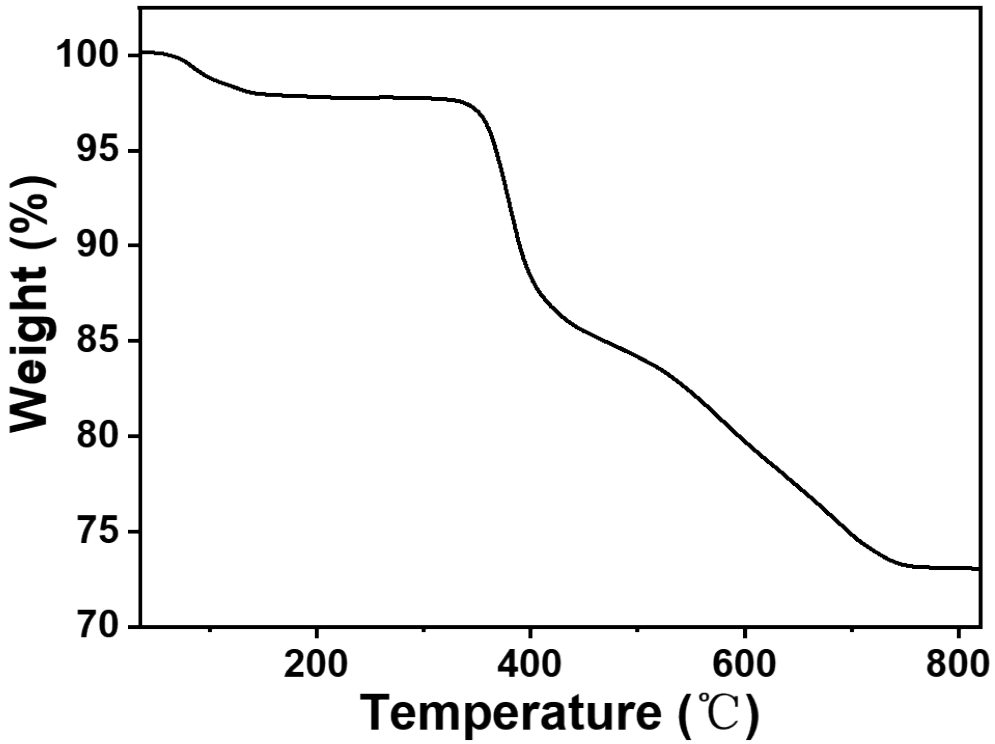

Fig. S11 The TG curve for **Co-ε-Keggin.**

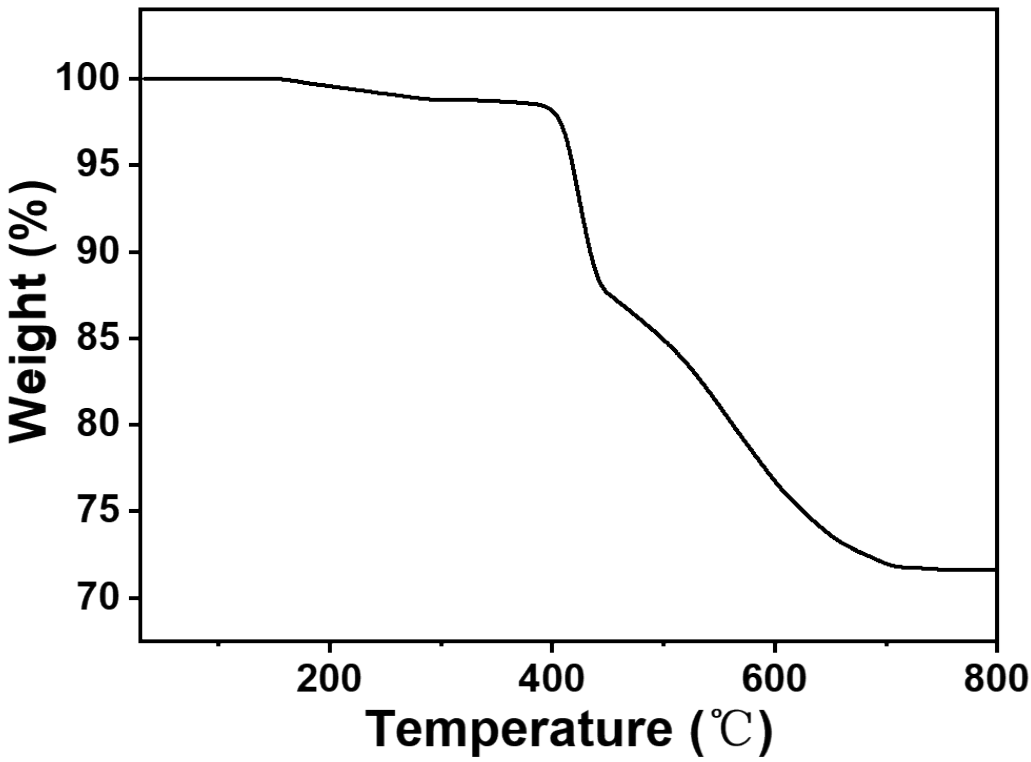

Fig. S12 The TG curve for **Ni-ε-Keggin.**

4.5 XPS

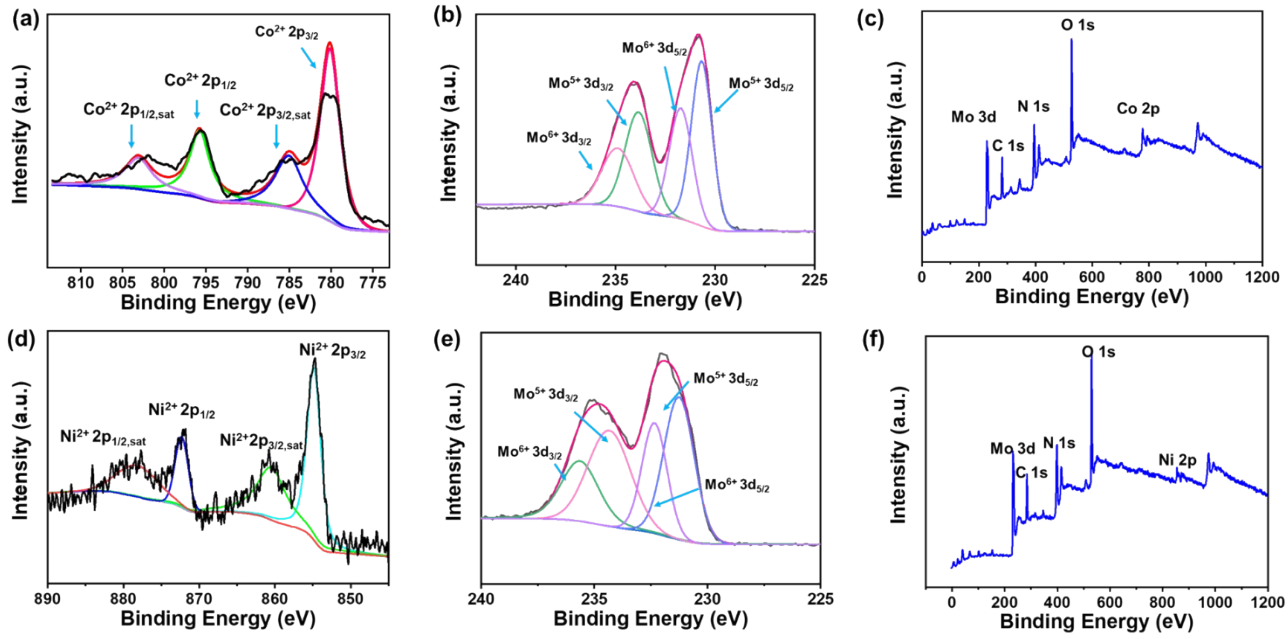

Fig. S13 (a) Co 2p spectrum analysis of **Co-ε-Keggin**. (b) Mo 3d spectrum analysis of **Co-ε-Keggin**. (c) Full spectrum analysis of **Co-ε-Keggin**. (d) Ni 2p spectrum analysis of **Ni-ε-Keggin**. (e) Mo 3d spectrum analysis of **Ni-ε-Keggin**. (f) Full spectrum analysis of **Ni-ε-Keggin**.

5. Photocatalytic CO_2 reduction experiments

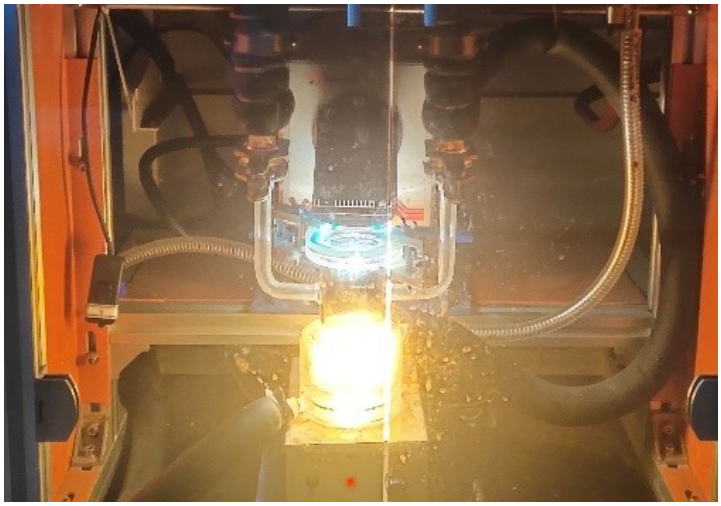

Fig. S14 The photograph of the CO_2 photoreduction devices.

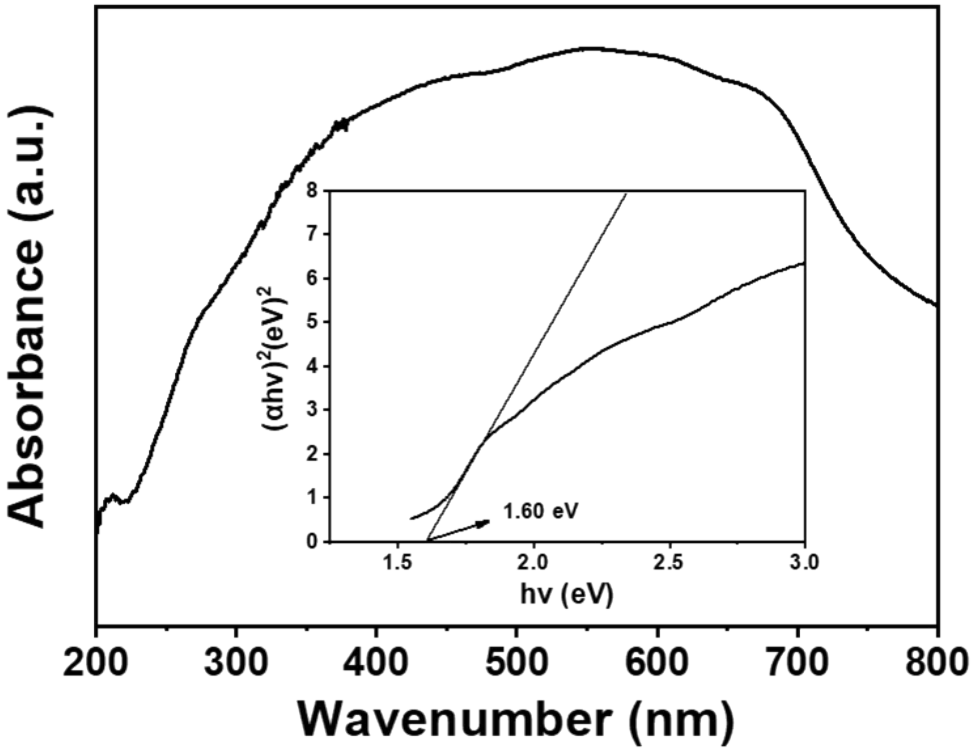

Fig. S15 UV/vis spectra, K-M function curves of **Co-ε-Keggin.**

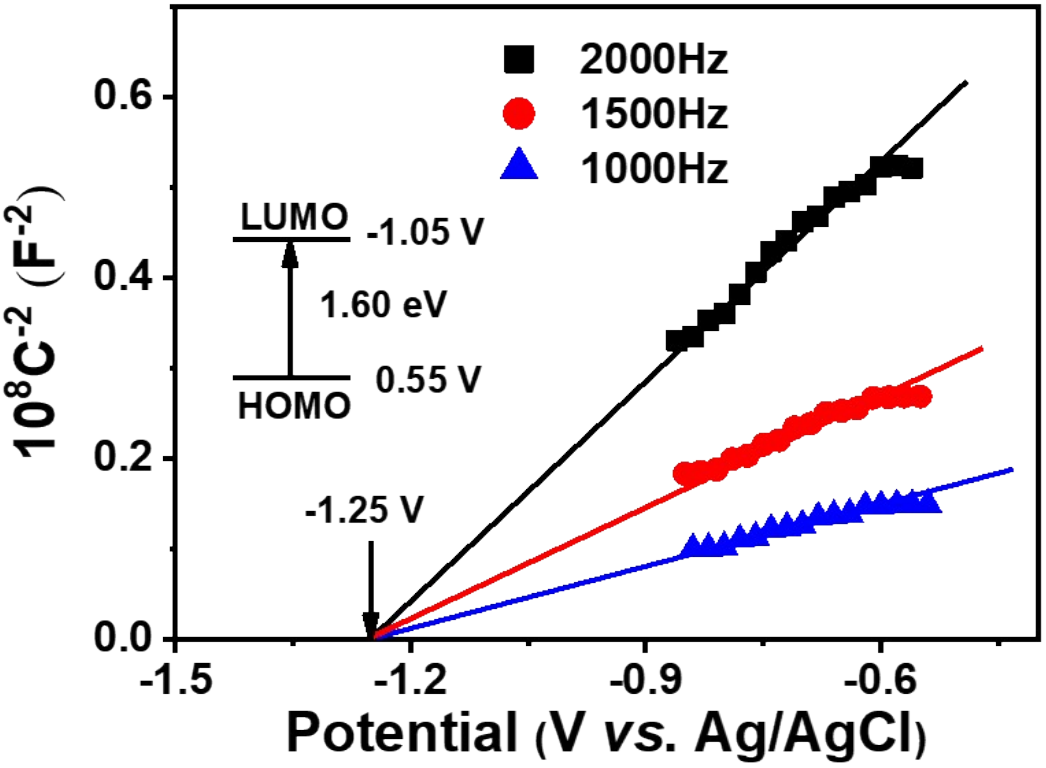

Fig. S16 Mott-Schottky plots for catalysts **Co-ε-Keggin**.

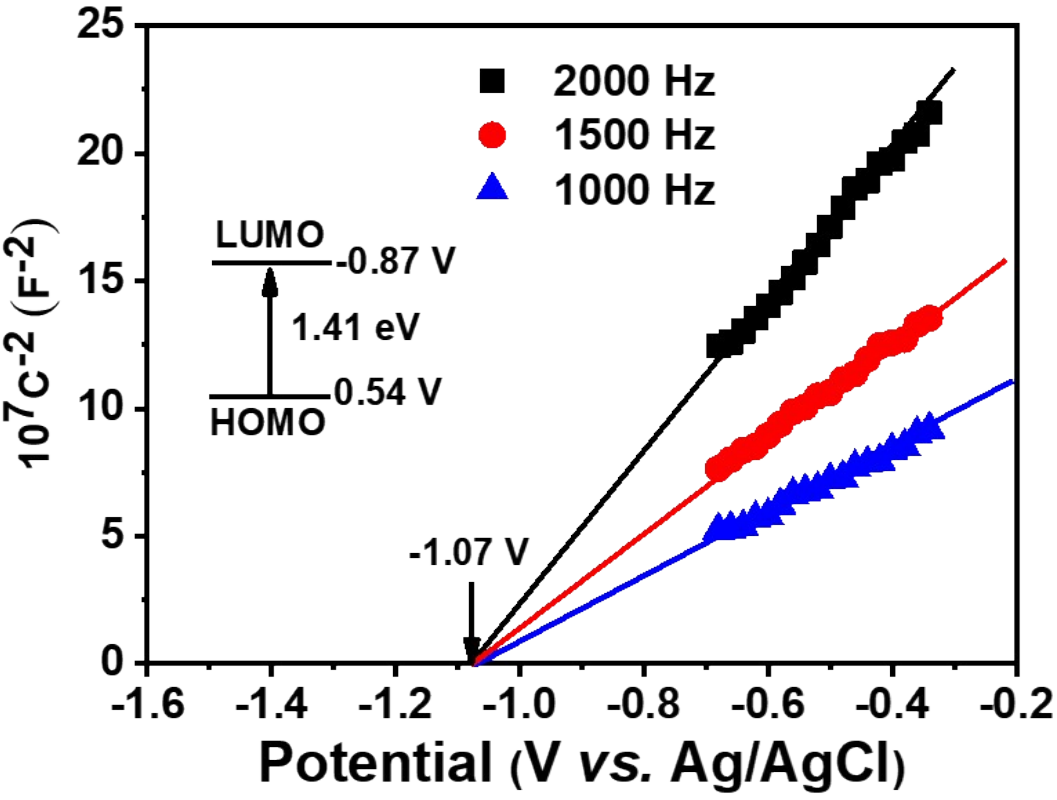

Fig. S17 Mott-Schottky plots for catalysts **Ni-ε-Keggin**.

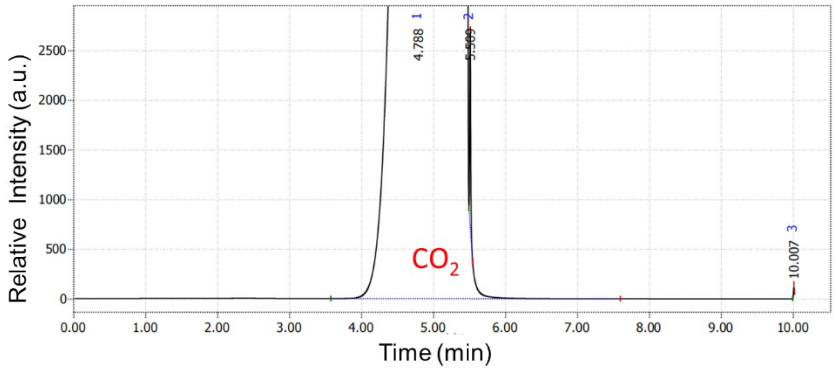

Fig. S18 GC profiles of CO_2 reduction to CO without light.

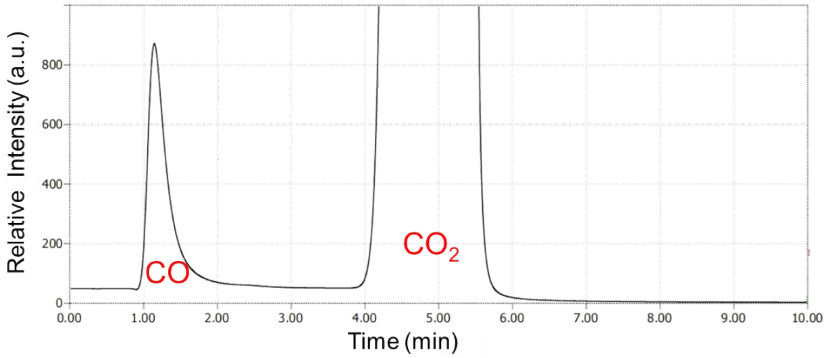

Fig. S19 GC profiles of 10% CO_2 reduction to CO with **Ni-ε-Keggin** as catalyst after reaction 6 h.

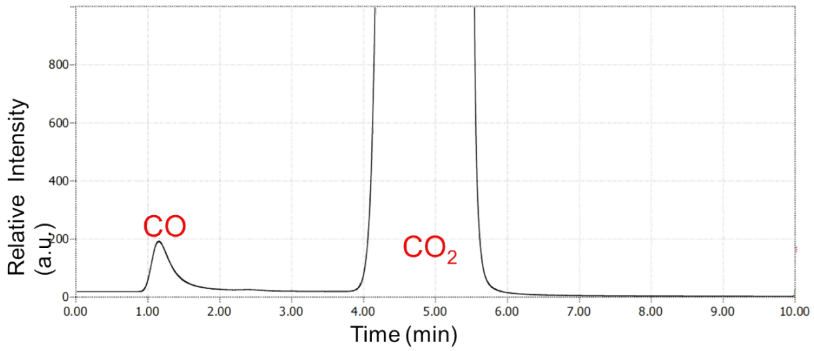

Fig. S20 GC profiles of 10% CO_2 reduction to CO with **Co-ε-Keggin** as catalyst after reaction 6 h.

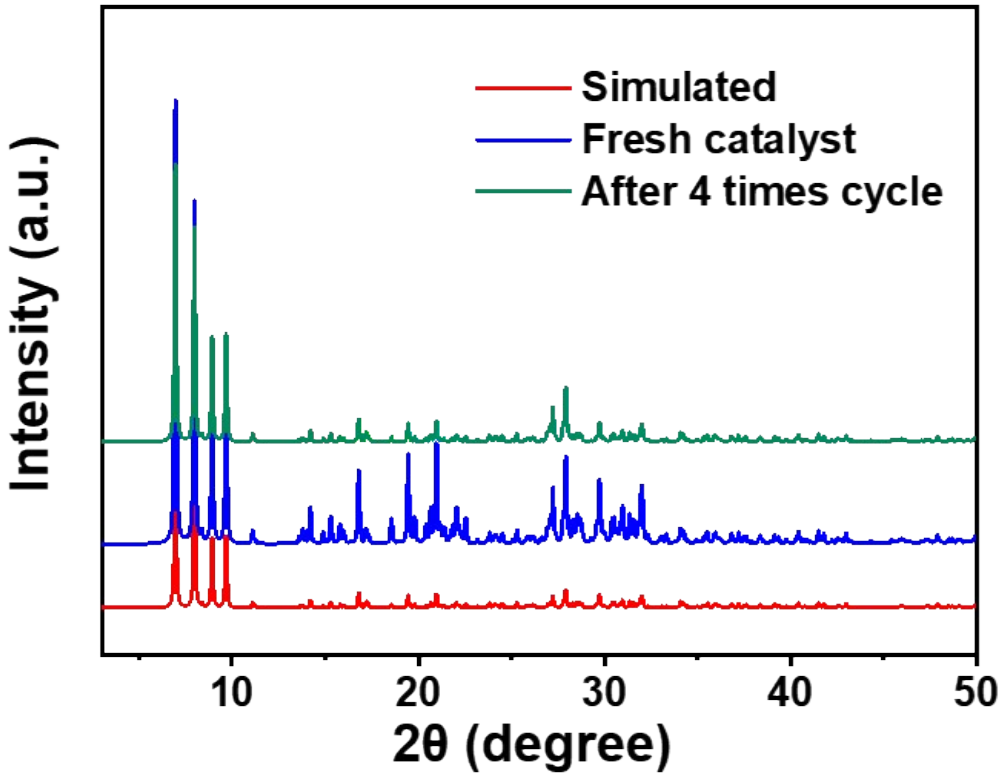

Fig. S21 PXRD patterns of **Co-ε-Keggin** before and after CO_2RR.

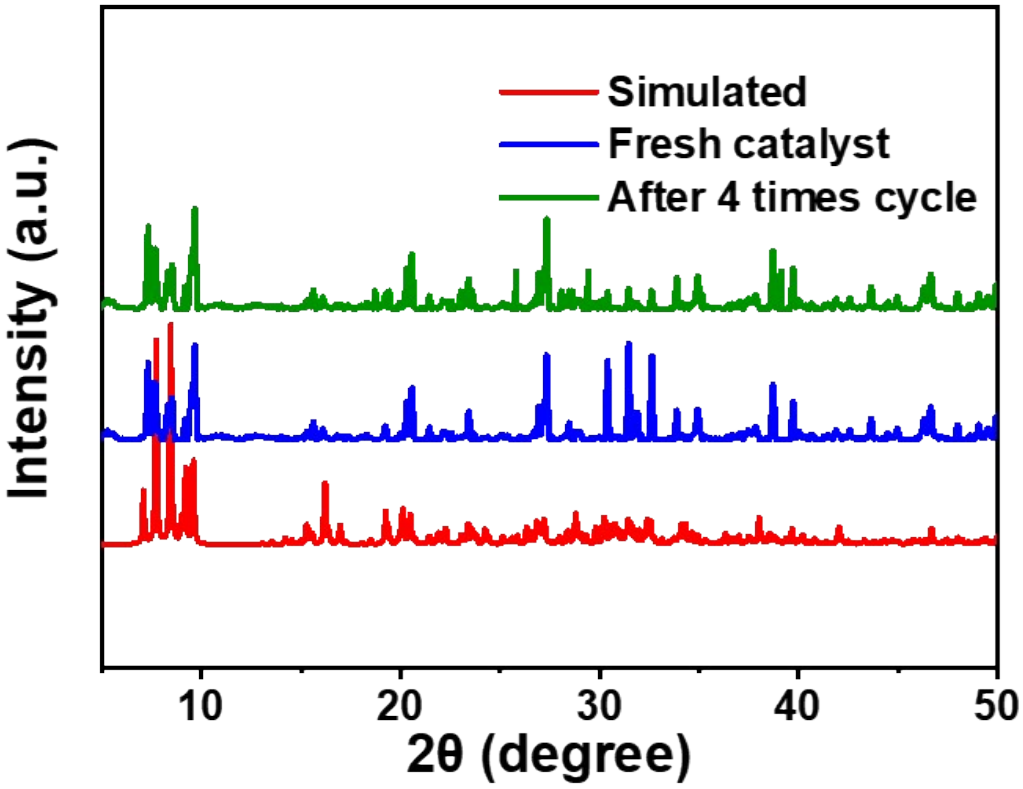

Fig. S22 PXRD patterns of **Ni-ε-Keggin** before and after CO_2RR.

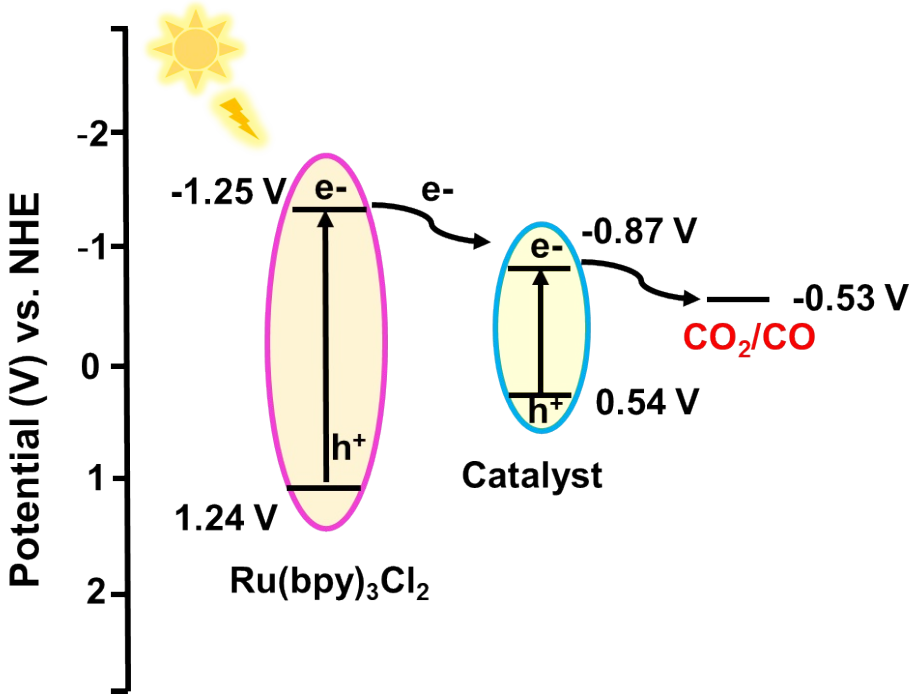

Fig. S23 Z- scheme diagram of the electron transfer process by using **Ni-ε-Keggin** as photocatalyst.

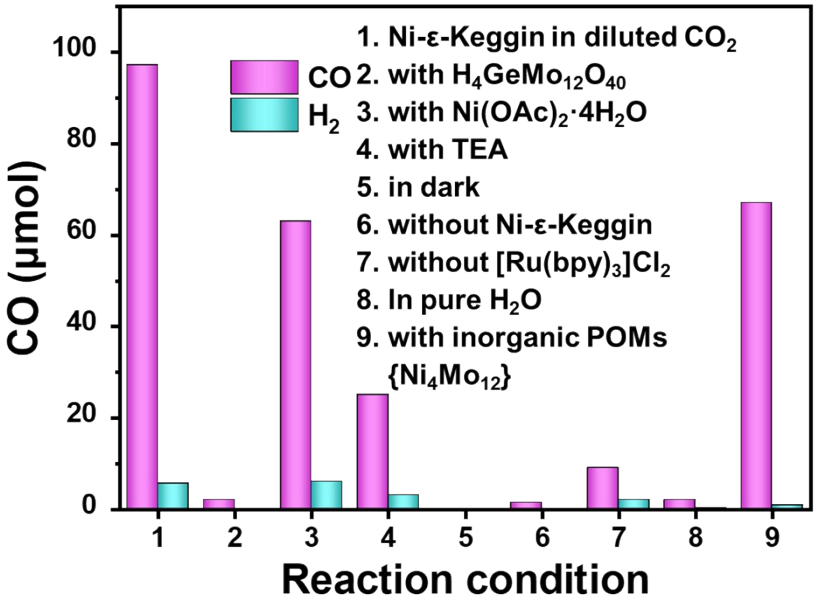

Fig. S24 Comparison of the activity of the photocatalytic CO_2RR under different conditions when catalyst **Ni-ε-Keggin** was used.

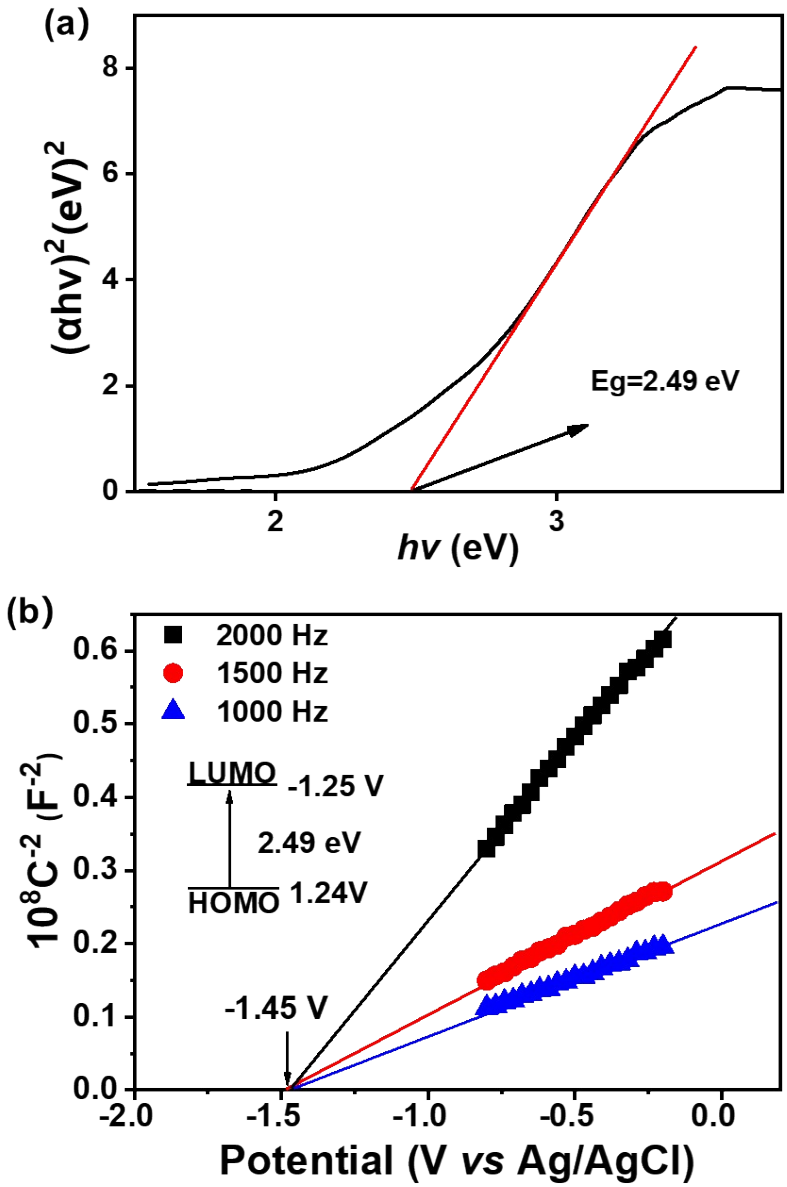

Fig. S25 (a) K-M function curves of $[Ru(bpy)_3]Cl_2$. (b)Mott-Schottky plots for $[Ru(bpy)_3]Cl_2$.

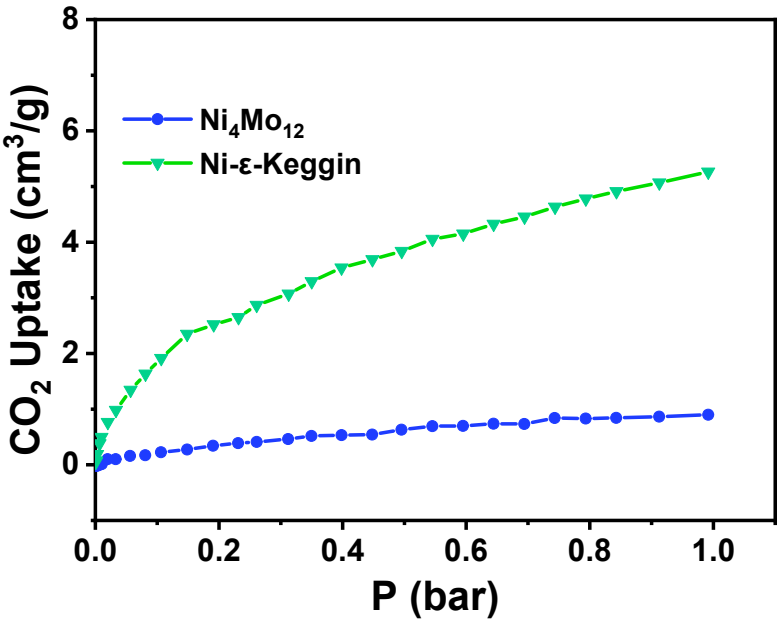

Fig. S26 CO_2 adsorption isotherms (298 K) of **{Ni_4Mo_{12}}** and **Ni-ε-Keggin** materials.

6. Table

Table S1. Comparison of reported POM-based hybrid materials photocatalyst for pure CO_2 to CO conversion.

Photocatalyst	**Photosensitizer** **Sacrificial agent**	**$Rate_{co}$** **(μmol g^{-1} h^{-1})**	**t**	**Selectivity** **CO (%)**	**Ref.**
Co-ε-Keggin	$[Ru(bpy)_3]Cl_2·6H_2O$ triethanolamine	7699.5	6h	96.5	This work
Ni-ε-Keggin	$[Ru(bpy)_3]Cl_2·6H_2O$ triethanolamine	24657.2	6h	98.3	This work
$H_{26.5}K_{2.5}Na(H_2O)_{16}[Ni_6(OH)(BO_3)_2(dien)_2(B\text{-}α\text{-}SiW_{10}O_{37})_2]_2·24H_2O$	$[Ru(bpy)_3]Cl_2·6H_2O$ triethanolamine	6988	1h	83.03	[1]
$[Co(en)_2]_6[V_{12}B_{18}O_{54}(OH)_6]·17H_2O$	$[Ru(bpy)_3]Cl_2·6H_2O$ triethanolamine	5700	3h	60	[2]
$(H_2bbi)_2\{[Co_2(bbi)][Co_{2.33}(H_2O)_4][H_{9.33}CoP_8Mo_{12}O_{62}]\}·4H_2O$	$[Ru(bpy)_3]Cl_2·6H_2O$ triethanolamine	3261	8h	-	[3]
$[Co_{2.67}(SiW_{12}O_{40})(H_2O)_4(Htrz)_4]·C_{11.33}$	$[Ru(bpy)_3]Cl_2·6H_2O$ triethanolamine	5235	6h	52	[4]
$(C_{11}NH_{10})_2\{[Co(H_2O)_6]@$	$[Ru(bpy)_3]Cl_2·6H_2O$	6764.3	8h	96.89	[5]

$[H_{29}Co_{16}Mo_{16}(H_2O)_{16}(PO_4)_{24}O_{36}]\}(H_2PO_4)\cdot 25H_2O$	triethanolamine				
$[Co_4(PO_4)(C_7H_8N_4)_6][BW_{12}O_{40}]\cdot 1.5H_2O$	$[Ru(bpy)_3]Cl_2\cdot 6H_2O$ triethanolamine	10852	5h	93.4	[6]

Table S2. Comparison of reported photocatalyst materials for 10% diluted CO_2 to CO conversion.

Photocatalyst	**CO_2 (vol%)**	**Photosensitizer Sacrificial agent**	**$Rate_{co}$**	**TOF (10^{-3})s^{-1}**	**SelectivityCO (%)**	**Ref.**
Co-ε-Keggin	10	$[Ru(bpy)_3]Cl_2\cdot 6H_2O$ TEOA	3496.0 (μmol g^{-1} h^{-1})	2.5	18.4	This work
Ni-ε-Keggin	10	$[Ru(bpy)_3]Cl_2\cdot 6H_2O$ TEOA	16199.3 (μmol g^{-1} h^{-1})	11.7	94.6	This work
COF-367-Co NS	10	$Ru(bpy)_3^{2+}$ ascorbic acid	2.587 mmol·g^{-1} h^{-1}	/	72	[7]
Ni@TPHH-COF	10	$Ru(bpy)_3^{2+}$ TEOA	3.28 mmol·g^{-1} h^{-1}	/	95	[8]
Ni-MOF1	10	$Ru(bpy)_3^{2+}$ TEOA	23.13 mmol g^{-1}	/	84.3	[9]
Ni MOLs	10	$Ru(bpy)_3^{2+}$ TEOA	12.5 (μmol/h)	/	96.8	[10]
Co MOLs	10	$Ru(bpy)_3^{2+}$ TEOA	0.44 (μmol/h)	/	9.6	[10]
Ni-TpBpy	10	$[Ru(bpy)_3]Cl_2$/ TEOA	915 μmol g^{-1}	/	76	[11]
COF-367-Co NSs	10	$[Ru(bpy)_3]Cl_2$/ TEOA	2875 (μmol g^{-1} h^{-1})	/	72	[12]
[Emim]BF4(56.41 wt%)@Zn-S-COF	15	/	105.88 (μmol g^{-1} h^{-1})	/	/	[13]
MAF-X27l-Cl	10	$[Ru(bpy)_3]Cl_2$/ TEOA	/	12	66.7	[14]
MAF-X27-OH	10	$[Ru(bpy)_3]Cl_2$/ TEOA	/	28	97.2	[14]
MAF-X27l-OH	10	$[Ru(bpy)_3]Cl_2$/ TEOA	/	59	98.2	[14]
MAF-X27-Cl	10	$[Ru(bpy)_3]Cl_2$/ TEOA	/	6.3	63.6	[14]
$[Co_2\text{-}(OH)L_1](ClO_4)_3$	10	$[Ru(bpy)_3](PF_6)_2$/ TEOA	/	9.5	92.0	[15]
Ru(II)-Re(I) dinuclear complex	10	BIH	/	16.7	100	[16]

Table S3. Selected bond lengths (Å) for **Co-ε-Keggin**.

Ge(1)-O(1)#1	1.781(7)	Ge(1)-O(1)	1.781(7)
Ge(1)-O(7)#1	1.787(7)	Ge(1)-O(7)	1.787(7)
Mo(1)-O(20)	1.683(8)	Mo(1)-O(4)	1.921(8)
Mo(1)-O(4)#1	1.948(8)	Mo(1)-O(11)	2.024(8)
Mo(1)-O(16)#1	2.117(7)	Mo(1)-O(7)#1	2.301(7)
Mo(2)-O(9)	1.702(8)	Mo(2)-O(13)	1.847(7)
Mo(2)-O(11)	1.848(8)	Mo(2)-O(2)	1.978(8)
Mo(2)-O(12)	1.988(8)	Mo(2)-O(7)#1	2.420(7)
Mo(3)-O(19)	1.676(8)	Mo(3)-O(6)	1.949(8)
Mo(3)-O(5)	1.957(8)	Mo(3)-O(15)	2.022(8)
Mo(3)-O(8)	2.105(8)	Mo(3)-O(1)#1	2.312(7)
Mo(4)-O(10)	1.738(8)	Mo(4)-O(15)	1.815(8)
Mo(4)-O(18)	1.834(8)	Mo(4)-O(2)	1.991(8)
Mo(4)-O(12)	2.002(8)	Mo(4)-O(1)#1	2.395(7)
Mo(5)-O(17)	1.683(9)	Mo(5)-O(3)#1	1.952(8)
Mo(5)-O(3)	1.953(8)	Mo(5)-O(18)#1	2.019(8)
Mo(5)-O(8)#1	2.077(8)	Mo(5)-O(1)	2.357(8)
Mo(6)-O(14)	1.673(8)	Mo(6)-O(5)	1.931(8)
Mo(6)-O(6)	1.973(7)	Mo(6)-O(13)#1	2.043(7)
Mo(6)-O(16)	2.112(8)	Mo(6)-O(7)	2.294(7)
Co(1)-O(6)	2.065(8)	Co(1)-O(2)	2.141(8)
Co(1)-N(6)	2.144(10)	Co(1)-N(4)	2.145(10)
Co(1)-N(5)	2.155(10)	Co(1)-O(4)	2.165(8)

Co(2)-O(3)#1	2.083(8)	Co(2)-O(5)#1	2.104(8)
Co(2)-N(1)	2.123(11)	Co(2)-N(2)	2.135(10)
Co(2)-O(12)	2.145(8)	Co(2)-N(3)	2.168(11)

Table S4. Selected bond lengths (Å) for **Ni-ε-Keggin**.

Ge(1)-O(16)	1.772(5)	Mo(5)-O(8)	1.971(4)
Ge(1)-O(6)	1.772(5)	Mo(5)-O(6)	2.357(4)
Ge(1)-O(3)#1	1.777(4)	Mo(6)-O(24)	1.692(4)
Ge(1)-O(3)	1.777(4)	Mo(6)-O(12)	1.918(4)
Mo(1)-O(19)	1.689(6)	Mo(6)-O(15)	1.954(4)
Mo(1)-O(4)#1	1.949(4)	Mo(6)-O(13)	1.965(5)
Mo(1)-O(4)	1.949(4)	Mo(6)-O(5)	1.967(4)
Mo(1)-O(18)	2.074(4)	Mo(6)-O(3)	2.360(4)
Mo(1)-O(18)#1	2.074(4)	Ni(1)-O(2)	2.049(5)
Mo(1)-O(16)	2.316(6)	Ni(1)-N(4)	2.071(7)
Mo(2)-O(17)	1.696(6)	Ni(1)-N(3)	2.092(6)
Mo(2)-O(4)#1	1.951(4)	Ni(1)-N(3)#1	2.092(6)
Mo(2)-O(4)	1.951(4)	Ni(1)-O(5)#1	2.143(4)
Mo(2)-O(14)#1	2.056(4)	Ni(1)-O(5)	2.143(4)
Mo(2)-O(14)	2.056(4)	Ni(2)-O(1)	2.066(6)
Mo(2)-O(6)	2.309(5)	Ni(2)-N(1)	2.076(8)
Mo(3)-O(22)	1.692(4)	Ni(2)-N(2)	2.102(6)
Mo(3)-O(11)	1.936(3)	Ni(2)-N(2)#1	2.102(6)
Mo(3)-O(5)	1.938(4)	Ni(2)-O(9)	2.109(4)
Mo(3)-O(13)	1.949(5)	Ni(2)-O(9)#1	2.109(4)

Mo(3)-O(18)	1.964(4)	Mo(4)-O(21)	1.685(4)
Mo(3)-O(16)	2.354(4)	Mo(4)-O(12)	1.937(4)
Mo(4)-O(8)	1.946(4)	Mo(4)-O(7)	1.958(4)
Mo(4)-O(9)	1.951(4)	Mo(4)-O(3)	2.345(4)
Mo(5)-O(23)	1.682(4)	Mo(5)-O(9)	1.957(4)
Mo(5)-O(10)	1.940(3)	Mo(5)-O(14)	1.968(4)

Table S5. Bond valence calculation (BVC) for **Co-ε-Keggin**.

Mo1	Mo2	Mo3	Mo4	Mo5	Mo6
4.94	5.20	4.87	5.90	4.86	4.90

Table S6. Bond valence calculation (BVC) for **Ni-ε-Keggin**.

Mo1	Mo2	Mo3	Mo4	Mo5	Mo6
4.80	4.83	4.99	5.76	4.94	4.88

X-ray crystallography

Select the crystal type and good quality crystal and glue it to the capillary glass tube. At 298 K, the crystallographic data of crystals **Co-ε-Keggin** and **Ni-ε-Keggin** were collected using Mo-Kα rays (λ = 0.71073 A) using Bruker Apex II CCD diffractometer in θ mode. The crystal structure of the compound was analyzed by the direct method using the SHELXL-2018/3 software package and refined by the least square method F^2.

Table S7. Partial crystallographic data and structural refinement of **Co-ε-Keggin** and **Ni-ε-Keggin**.

Compound	**Co-ε-Keggin**	**Ni-ε-Keggin**
Formula	$C_{16}H_{66}Co_4GeMo_{12}N_{12}O_{45}$	$C_{16}H_{64}GeMo_{12}N_{12}Ni_4O_{44}$
Formula weight	2606.39	2587.50
T (K)	293 (2)	293 (2)
Crystal system	Monoclinic	Monoclinic

Space group	*C*2/*c*	P 21/m
a (Å)	16.107(7)	12.829(3)
b (Å)	21.036(7)	18.764(5)
c (Å)	18.501(7)	13.571(3
β (°)	98.575(6)°	90°
V (Å^3)	6199(4)	3111.9(13)
Z	4	2
D_c (mg m^{-3})	2.793	2.761
μ (mm^{-1})	3.958	4.084
F (000)	5000	2488
θ range (°)	1.575-7.213	1.575-27.213
Crystal size (mm^3)	0.15×0.14×0.12	0.13×0.12×0.10
Limiting indices	-19≤*h*≤17, -24≤*k*≤25, -22≤*l*≤22	-15≤*h*≤15 -22≤*k*≤22, -16≤*l*≤16
Reflections collected	20263	22394
R(int)	0.0822	0.1024
Data / restraints / parameters	5463/65/411	5694/65/437
GOF on F^2	1.158	1.052
$R_1{}^a$, $wR_2{}^b$ [$I > 2\sigma(I)$]	R1=0.0639, wR2=0.1374	R1=0.0458, wR2=0.1229
R_1, wR_2 (all data)	R1=0.0779, wR2=0.1421	R1=0.0538, wR2=0.1287

7. Theoretical calculations

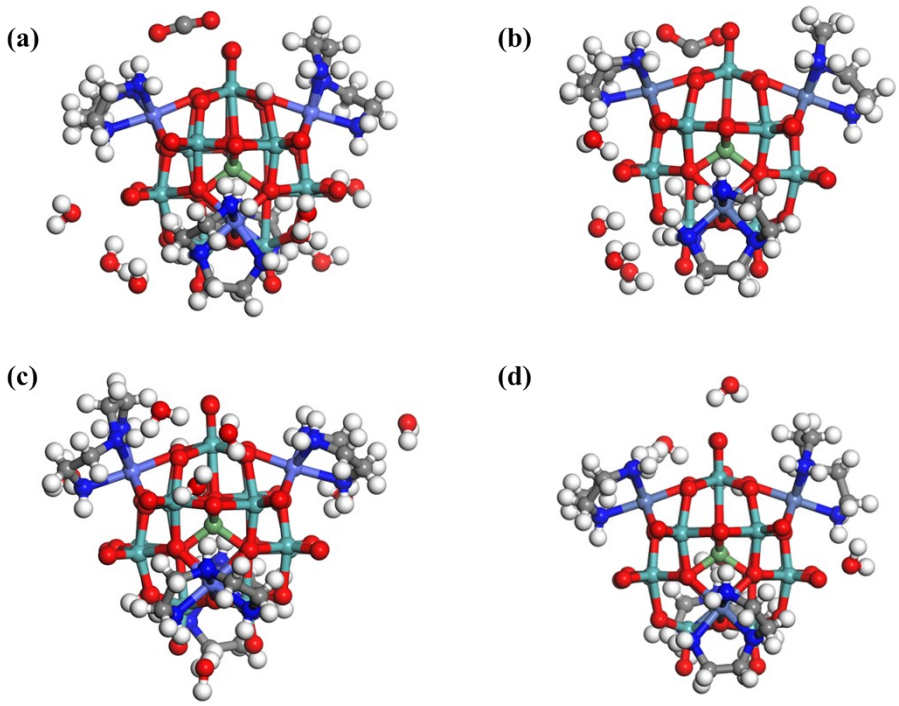

Fig. S27 (a) DFT-derived CO_2 binding structures of catalyst **Co-ε-Keggin.** (b) DFT-derived CO_2 binding structures of catalyst **Ni-ε-Keggin**. (c) DFT-derived H_2O binding structures of catalyst **Co-ε-Keggin.** (d) DFT-derived H_2O binding structures of catalyst **Ni-ε-Keggin**.

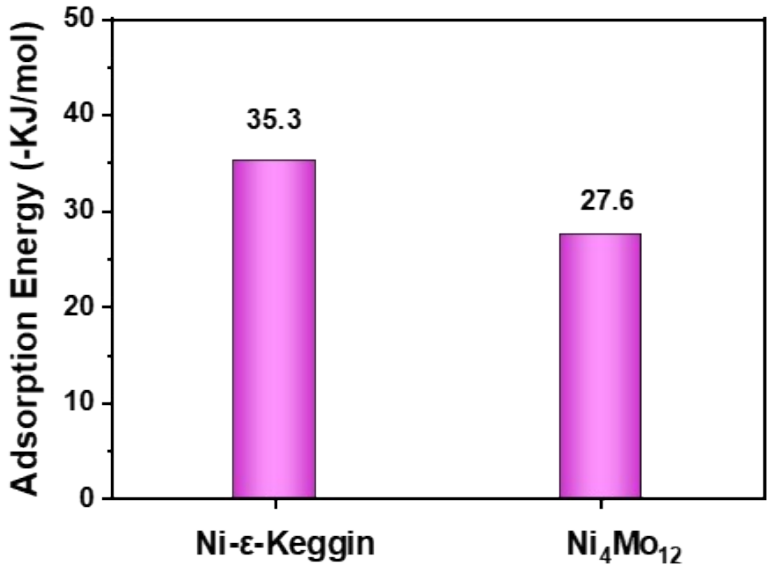

Fig. S28 The adsorption energies of CO_2 for **Ni-ε-Keggin** and **Ni_4Mo_{12}** were compared.

8. References

[1] Y. Chen, Z.-W. Guo, Y.-P. Chen, Z.-Y. Zhuang, G.-Q. Wang, X.-X. Li, S.-T. Zheng and G.-Y. Yang, *Inorg. Chem. Front.,* 2021, **8**, 1303−1311.

[2] X. Yu, C.-C. Zhao, J.-X. Gu, C.-Y. Sun, H.-Y. Zheng, L.-K. Yan, M. Sun, X. L. Wang and Z.-M. Su, *Inorg. Chem.,* 2021, **60**, 7364−7371.

[3] J.-N. Li, Z.-Y. Du, N.-F. Li, Y.-M. Han, T.-T. Zang, M.-X. Yang, X.-M. Liu, J.-L. Wang, H. Mei and Y. Xu, *Dalton Trans.,* 2021, **50**, 9137−9143.

[4] W. Yao, C. Qin, N. Xu, J. Zhou, C. Sun, L. Liu and Z. Su, *CrystEngComm.,* 2019, **21**, 6423−6431.

[5] C. Li, H.-Y. Jiang, J.-L.Wang, R.-K. Kang, H. Mei and Y. Xu, *Dalton Trans.,* 2022, **51**, 9616−9621.

[6] Z.-Y. Du, Y.-N. Xue, X.-M. Liu, N.-F. Li, J.-L. Wang, H. Mei and Y. Xu, *J. Mater. Chem. A,* 2022, **10**, 3469−3477.

[7] W. Liu, X. Li, C. Wang, H. Pan, W. Liu, K. Wang, Q. Zeng, R. Wang and J. Jiang, *J. Am. Chem. Soc.,* 2019, **141**, 17431−17440.

[8] M. Dong, J. Zhou, J. Zhong, H. T. Li, C. Y. Sun, Y. D. Han, J. N. Kou, Z. H. Kang, X. L. Wang and Z. M. Su, *Adv. Funct. Mater*., 2022, **32**, 2110136.

[9] M. Dong, Y. Tian, J.-X.Gu, X.-H. Wang, L.-X. Wang, B.-S. Hou, A. Yousuf, C.-Y. Sun, J. Wu, Z.-H. Kang, X.-L. Wang and Z.-M. Su, *Inorg. Chem. Front.,* 2023, **10**, 1279−1285.

[10] B. Han, X. Ou, Z. Deng, Y. Song, C. Tian, H. Deng, Y. J. Xu and Z. Lin, *Angew. Chem. Int. Ed.*, 2018, **57**, 16811−16815.

[11] W. Zhong, R. Sa, L. Li, Y. He, L. Li, J. Bi, Z. Zhuang, Y. Yu and Z. Zou, *J. Am. Chem. Soc.,* 2019, **141**, 7615-7621.

[12] W. Liu, X. Li, C. Wang, H. Pan, W. Liu, K. Wang, Q. Zeng, R. Wang and J. Jiang, *J. Am. Chem. Soc.,* 2019, **141**, 17431-17440.

[13] Y. Yang, H.-Y. Zhang, Y. Wang, L.-H. Shao, L. Fang, H. Dong, M. Lu, L.-Z. Dong, Y.-Q. Lan and F.-M. Zhang, *Adv Mater*., 2023, 2304170.

[14] Y. Wang, N.-Y. Huang, J.-Q. Shen, P.-Q. Liao, X.-M. Chen and J.-P. Zhang, *J. Am. Chem. Soc*., 2018, **140**, 38–41.

[15] T. Ouyang, H. H. Huang, J. W. Wang, D. C. Zhong, T. B. Lu, *Angew. Chem. Int. Ed*., 2017, **56**, 756–761.

[16] T. Nakajima, Y. Tamaki, K. Ueno, E. Kato, T. Nishikawa, K. Ohkubo, Y. Yamazaki, T. Morimoto and O. Ishitani, *J. Am. Chem. Soc*., 2016, **138**, 13818–13821.

[17] A. Mueller, C. Beugholt, P. Koegerler, H. Bo1gge, S. Bud'ko and M. Luban. *Inorg. Chem*., 2000, **23**, 5176–5177.